Available online at www.rsu.ac.th/rjas

Rangsit Journal of Arts and Sciences, January-June 2016 RJAS Vol. 6 No. 1, pp. 1-16
Copyright © 2011, Rangsit University
ISSN2229-063X (Print)/ISSN2392-554X (Online)
DOI : 10.14456/rjas.2016.1

A performance impact of Andrew's Sine threshold for a robust regularized SRR based on ML framework

Vorapoj Patanavijit[1*] and Kornkamol Thakulsukanant[2]

[1]Department of Electrical and Electronic Engineering, Vincent Mary School of Engineering, Assumption University of Thailand, Samuthprakarn 10540, Thailand
[2]Department of Business Information Systems, Martin de Tours School of Management and Economics, Assumption University of Thailand, Samuthprakarn 10540, Thailand
E-mail: Patanavijit@yahoo.com, E-mail: kthakulsukanan@yahoo.com
[*]Corresponding author

Submitted 20 July 2015; accepted in final form 1 December 2015
Available online 21 June 2016

Abstract

One of the most successful Digital Image Reconstruction (DIR) techniques for increasing image resolution and improving image quality is the Super-Resolution Reconstruction (SRR), which is the procedure of integrating a collection of aliased low-resolution low-quality images to form a single high-resolution high-quality image. However, the mainstream SRR algorithms are too delicate to noisy environments because these mainstream SRR algorithms are often comprised by the ML (L1 or L2) estimation techniques thereby the new robust SRR algorithm, which is comprised by Andrew's Sine norm, has been proposed for dealing with noisy environments. Because the performance of the new SRR algorithm heavily relies on this Andrew's Sine norm soft-threshold parameter, resultantly, this paper aims to investigate the impact characteristic of this norm constant parameter on the novel SRR algorithm. In addition, multitudinous experiments (which are applied on two standard images: Lena image and Susie image) are simulated to make the extensive results under five noise models: noise free, additive Gaussian noise, multiplicative Gaussian noise, Poisson noise and Impulsive noise with several noise powers for demonstrating the relationship between the SRR performance (in PSNR) and Andrew's Sine norm soft-threshold parameter under each noisy cases.

Keywords: *SRR (Super-Resolution Reconstruction), DIR (Digital Image Reconstruction), DIP (Digital Image Processing), ML (Maximum Likelihood) Estimation, DSP (Digital Signal Processing)*

1. Correlatively researched works

In the past twenty years, a large-scale diversity of SRR algorithms, which is a successful reconstructed technique for increasing optical resolution and improving image quality (Ng & Bose, 2003; Kang & Chaudhuri, 2003; Rajan, Chaudhuri, & Joshi, 2003; Park, Park, & Kang, 2003), have been studied and enquired (Farsiu, Robinson, Elad, & Milanfar, 2004a; Patanavijit, 2009a) for a catalogue of representatives of this enormous researched reviews.

From the estimation technique prospective, almost all these mainstream SRR algorithms (Patanavijit, 2009b) are often comprised by the L1 Norm estimation technique (Farsiu, Robinson, Elad, & Milanfar, 2004b; Farsiu, Elad, & Milanfar, 2006) and the L2 Norm estimation technique (Schultz & Stevenson, 1994; Schultz & Stevenson, 1996; Elad & Feuer, 1997; Elad & Feuer, 1999a; Elad & Feuer, 1999b; Elad & Hel-Or, 2001) to be the fidelity term in the mathematical error function. For additive Gaussian noisy environments, the L1 Norm estimation technique often provides the estimated result with greater error range than the L2 Norm estimation technique. Nevertheless, the L2 Norm estimation technique is too delicate to non-Gaussian or Impulsive noisy environments than the L1 Norm estimation technique. From the robust signal processing prospective (Black, Sapiro, Marimont, & Heeger, 1998), one of the robust norm estimation techniques is Andrew's Sine norm, which is invented for resisting non-Gaussian or Impulsive noise. For norm estimation characteristic prospective, the Andrew's Sine norm is mathematically similar to the L2 norm estimation technique for low-power noise or low-power outlier but the Andrew's Sine norm is mathematically similar to the L1 norm estimation technique for high-power noise or high-power outlier, instead. Consequently, the new robust SRR algorithm (Patanavijit, 2008; Patanavijit, 2009c, Patanavijit, 2015), which is comprised by Andrew's Sine norm, has been proposed for

observed synthesized low-optical resolution low-quality images in 2008 and it has the better performance for dealing with noisy environments than these previous mainstream SRR algorithms, which is comprised by L1 and L2 norm estimation techniques. Later, the new robust SRR algorithm (Patanavijit, 2009d), which is comprised by Andrew's Sine norm, for low-optical resolution low-quality videos has been proposed in 2009. Next, the new robust SRR algorithm (Patanavijit, 2011), which is comprised by Andrew's Sine norm and fast affine block-based registration, for low-optical resolution low-quality videos has been proposed in 2011. Nevertheless, the performance of the new robust SRR algorithm with Andrew's Sine norm is heavily relies on this Andrew's Sine norm soft-threshold parameter thereby this paper aims to investigate the impact characteristic of this norm constant parameter on the novel SRR algorithm. Resultantly, under five noise models: noise free, additive Gaussian noise, multiplicative Gaussian noise, Poisson noise and Impulsive noise with several noise powers, multitudinous experiments, which are applied on two standard images: Lena image and Susie image, are simulated to make the extensive results for demonstrating the relationship between the SRR performance (in PSNR) and Andrew's Sine norm soft-threshold parameter under each noisy cases.

The alignment of this research article is as succeeding. The general conception of the mainstream SRR algorithm by the L1 or L2 estimation techniques is succinctly disclosed in Section 2. The novel conception of the robust SRR algorithm, which is implemented by regularized ML framework with Andrew's Sine estimation technique, is nominated in Section 3. Under various noise models, multitudinous experiments are simulated to make the extensive results for demonstrating the relationship between the SRR performance (in PSNR) and Andrew's Sine norm soft-threshold parameter under each noisy case in Section 4. Lastly, simulated consequence and argument are arranged in Section 5.

2. Conception of super-resolution reconstruction algorithm

Section 2 succinctly discloses the general conception of the mainstream SRR (Super-Resolution Reconstruction) algorithm by the L1 or L2 estimation (Elad & Feuer, 1999b; Elad & Hel-O, 2001; Patanavijit, 2008; Patanavijit, 2015). Mathematical designate that a group of aliased low optical resolution images are $\{\mathbf{Y}(t)\}$ as the discovered signals, which incorporates $N_1 \times N_2$ pixels and a single high optical resolution high-quality image is $\mathbf{X}(t)$ as the mathematical integrated fused signal, which incorporates $qN_1 \times qN_2$ pixels (where q the optical resolution increasing factor in both the straight and straight-up axis) and is mathematical integrated from group of aliased low optical resolution images $\{\mathbf{Y}(t)\}$

For scaling down the data processing memory, each image is detached into a small imbricate piece. From the mainstream of SRR notation, the small imbricate piece of image can be mathematical specified as vector form by using the column-wise lexicographically formatting. The small imbricate piece of aliased low optical resolution images can be mathematical specified as $\underline{Y}_k \in \mathbf{R}^{M^2}$, which incorporates $M^2 \times 1$ pixels and the small imbricate piece of high optical resolution image can be mathematical specified as $\underline{X} \in \mathbf{R}^{q^2M^2}$, which incorporates $L^2 \times 1$ or $q^2M^2 \times 1$ pixels. For the SRR prospective, these two small imbricate pieces of image are mathematically specified as succeeding equation

$$\underline{Y}_k = D_k H_k F_k \underline{X} + \underline{V}_k \quad ; k = 1, 2, \ldots, N \qquad (1)$$

where $\underline{X}$ is the small imbricate piece of the ground truth image (unknown), which can be mathematical specified in the vector format. $\underline{Y}_k$ is the aliased low optical resolution images, which can be mathematical specified in the vector format. F_k represents for the graphic misshape process, which is usually translation movement model, between the small imbricate piece $\underline{X}$ and $\underline{Y}_k$, which can be mathematical specified in the matrix format as $F \in \mathbf{R}^{q^2M^2 \times q^2M^2}$. H_k represents for the ocular blur process, which is usually spatial stable and time stable property, which can be mathematical specified in the matrix format as $H_k \in \mathbf{R}^{q^2M^2 \times q^2M^2}$. D_k represents for the optical resolution declining process, which is usually constant, which can be mathematical specified in the matrix format as $D_k \in \mathbf{R}^{M^2 \times q^2M^2}$. $\underline{V}_k$ represents for the noise in detection process, which can be mathematical specified in the vector format as $\underline{V}_k \in \mathbf{R}^{M^2}$.

From inverse problem prospective, the SRR problem (Farsiu et al., 2004b; Farsiu, Elad & Milanfar, 2006), which can be mathematical specified in Eq.(1), is classified as an ill-posed case. Therefore, an infinite number of estimated images ($\underline{X}$) make Eq. (1) correct in the under-determined situation or the estimated image ($\underline{X}$) will have a great error if there are a little noise in aliased low optical resolution images ($\underline{Y}_k$) in full-rank and over-determined cases. For solving this problem, the regularized technique (Patanavijit, 2009b) has been proposed for incorporating in SRR framework to prize the stable solution, to boost the convergence processing time and to discard artifacts in the estimated image ($\underline{X}$).

2.1 L1 Norm estimation for SRR algorithm based on ML framework

The L1 Norm estimation technique is the first robust norm estimator, which has been applied in the DSP fields, especially DIP. In 2004, the L1 Norm estimation technique has been first implemented in SRR framework (Farsiu, et al., 2004b; Farsiu, Elad & Milanfar, 2006). Because of ill-posed case in inverse problem, the regularized technique must be embodied with SRR framework for reimbursing the error or lost information as the ordinary prior function, which is typically modeled as an error function in this problem Maximum Likelihood error function. The Tiknonov regularized error function, which can be mathematically reduced to be Laplacian regularization (Farsiu, et al., 2004b), is one of the most uncomplicated and effective regularized technique therefore the Maximum Likelihood error function of this SRR problem can be mathematically specified as succeeding equation

$$\underline{X} = \underset{\underline{X}}{\text{ArgMin}} \left\{ \sum_{k=1}^{N} \left\| D_k H_k F_k \underline{X} - \underline{Y}_k \right\| + \lambda \cdot \left(\Gamma \underline{X} \right)^2 \right\} \quad (2)$$

where λ is the regularization constant the Laplacian kernel of Γ is mathematical specified as succeeding equation

$$\Gamma_{\text{KERNAL}} = 1/8 \begin{bmatrix} 1 & 1 & 1 \\ 1 & -8 & 1 \\ 1 & 1 & 1 \end{bmatrix} \quad (3)$$

By the steepest descent method (Patanavijit, 2013) for determining the minimized solution, the estimated image ($\underline{X}$) of problem (2) mathematically specified as succeeding equation

$$\hat{\underline{X}}_{n+1} = \hat{\underline{X}}_n + \beta \cdot \left\{ \begin{array}{l} \left(\sum_{k=1}^{N} F_k^T H_k^T D_k^T \operatorname{sign}\left(D_k H_k F_k \hat{\underline{X}}_n - \underline{Y}_k \right) \right) \\ -\left(\lambda \cdot \left(\Gamma^T \Gamma \right) \hat{\underline{X}}_n \right) \end{array} \right\} \quad (4)$$

where β is the step constant in the gradient descend method.

2.2 L2 Norm estimation for SRR algorithm based on ML framework

The L2 Norm estimation technique is the classical and the first norm estimator, which has been applied in the DSP fields, especially DIP. In 1994, the L2 Norm estimation technique has been first implemented in SRR framework (Schultz & Stevenson, 1994; Schultz & Stevenson, 1996). Combined with the Tiknonov regularized error function, the Maximum Likelihood error function of this SRR problem can be mathematically specified as succeeding equation

$$\underline{X} = \underset{\underline{X}}{\text{ArgMin}} \left\{ \sum_{k=1}^{N} \left\| D_k H_k F_k \underline{X} - \underline{Y}_k \right\|_2^2 + \lambda \cdot \left(\Gamma \underline{X} \right)^2 \right\} \quad (5)$$

By the steepest descent method (Patanavijit, 2013) for determining the minimized solution, the estimated image ($\underline{X}$) of problem (5) mathematically specified as succeeding equation

$$\hat{\underline{X}}_{n+1} = \hat{\underline{X}}_n + \beta \cdot \left\{ \begin{array}{l} \sum_{k=1}^{N} F_k^T H_k^T D_k^T \left(\underline{Y}_k - D_k H_k F_k \hat{\underline{X}}_n \right) \\ -\left(\lambda \cdot \left(\Gamma^T \Gamma \right) \hat{\underline{X}}_n \right) \end{array} \right\} \quad (6)$$

3. Andrew's Sine norm estimation for SRR algorithm based on ML framework

The Andrew's Sine norm estimation technique is one of the robust norm estimators (Black et al., 1998), which has been applied in the robust signal processing fields. For norm estimation characteristic prospective, the Andrew's Sine norm is similar to the L2 norm estimation technique for low-power noise or low-power outlier but the Andrew's Sine norm is similar to the L1 norm estimation technique for high-power noise or high-power outlier, instead. In 2008, the Andrew's Sine norm estimation technique has been first implemented in SRR framework (Patanavijit, 2008). Combined with the Tiknonov regularized error function, the Maximum Likelihood error function of this SRR problem can be mathematically specified as succeeding equation

$$\underline{X} = \underset{\underline{X}}{\text{ArgMin}} \left\{ \begin{array}{l} \sum_{k=1}^{N} f_{\substack{ANDREW \\ SINE}} \left(D_k H_k F_k \underline{X} - \underline{Y}_k \right) \\ +\lambda \cdot \left(\Gamma \underline{X} \right)^2 \end{array} \right\} \quad (7)$$

$$f_{\substack{ANDREW \\ SINE}}(x) = \begin{cases} \left(T^2 \right) \sin^2 \left(x/2T \right) & ;|x| \le \pi T \\ T^2 & ;|x| > \pi T \end{cases} \quad (8)$$

where T is Andrew's Sine norm constant parameter, which is a soft threshold real number.

By the steepest descent method (Patanavijit, 2013) for determining the minimized solution, the estimated image ($\underline{X}$) of problem (8) mathematically specified as succeeding equation

$$\underline{\hat{X}}_{n+1} = \underline{\hat{X}}_n + \beta \cdot \begin{Bmatrix} \sum_{k=1}^{N} F_k^T H_k^T D_k^T \cdot \underset{SINE}{\psi_{ANDREW}} \left(\underline{Y}_k - D_k H_k F_k \underline{\hat{X}}_n \right) \\ -\left(\lambda \cdot \left(\Gamma^T \Gamma \right) \underline{\hat{X}}_n \right) \end{Bmatrix} \quad (9)$$

$$\underset{SINE}{\psi_{ANDREW}}(x) = \underset{SINE}{f'_{ANDREW}}(x) = \begin{cases} T \sin(x/T) & ;|x| \le \pi T \\ 0 & ;|x| > \pi T \end{cases} \quad (10)$$

4. The data processing simulation issue

The purpose of this section is to analyze how the proposed robust norm estimation (Andrew's Sine norm) can affect the performance of the SRR algorithm (in PSNR). This section presents the experiments and results obtained the SRR algorithms using the proposed Andrew's Sine norm estimation technique compared with the previous SRR algorithms using the L1 norm estimation technique and L2 norm estimation technique.

These image processing simulations are written by MATLAB and the small imbricate piece of the aliased low optical resolution images ($\underline{Y}_k$) is appointed at 8x8 and the small imbricate piece of the ground truth image (unknown) ($\underline{X}$) is appointed at 16x16. This simulation processes the 40th frame Susie sequence (which is converted in the gray intensity with 176x144 in QCIF format) and the Lena (which is converted in the gray intensity with 256x256). Next, this simulation constitutes the aliased low optical resolution images ($\{\mathbf{Y}(t)\}$) by first translational graphic misshape processing this original HR image ($\mathbf{X}(t)$) by one pixel in the vertical axis and, second, ocular blur processing (which is usually spatial stable and time stable property) the graphic misshaped HR image and, third, optical resolution declining processing the ocular blurred graphic misshaped HR image and, forth, noise addition processing the ocular blurred graphic misshaped LR image $\{\mathbf{Y}(t)\}$ with contrasting noise models and noise power intensities. With contrasting translational graphic misshape in vertical and horizontal axis, the same simulation process was executed to constitute 4 aliased low optical resolution images ($\{\mathbf{Y}(t)\}$) from original HR image ($\mathbf{X}(t)$). All 4 aliased low optical resolution images ($\{\mathbf{Y}(t)\}$) are performed as the input images of a regularized SRR algorithm based on ML framework.

The guideline for selecting these simulated parameter: λ, β and n was for constituting the estimated image in both the most visual quality and the highest PSNR. Moreover, for making sure the honesty results, each simulations were replayed plentiful times with contrast parameter values and the estimated image with the most visual quality and the highest PSNR is selected. (Farsiu et al., 2004b; Farsiu, Elad, & Milanfar, 2006, Patanavijit, 2008).

4.1 The simulation of Andrew's Sine norm soft-threshold parameter

This section presents the simulation results of the optimized Andrew's Sine norm soft-threshold parameter (which is varied from 1 to 19), which make the SRR framework for constituting the estimated image in both the most visual quality and the highest PSNR as shown in Table 1 and Table 2 for Susie and Lena, respectively. These simulation results consist of 4 noise models as succeeding: Additive White Gaussian Noise (AWGN) at five power intensities as SNR=15, 17.5, 20, 22.5, 25dB, Poisson Noise at one power intensity, Multiplicative White Gaussian Noise (Speckle Noise) at three power intensities as V=0.01, 0.02, 0.03, Salt&Pepper Noise at three power intensities as D=0.005, 0.010, 0.015.

From the relationship between Andrew's Sine norm soft-threshold parameter and the PSNR of both the estimated Susie image as shown Table 1 (and Figure 1) and the estimated Lena image as shown Table 2 (and Figure 2), these comparatively simulated results are condensed as succeeding.

For AWGN and Poisson Noise, the Andrew's Sine norm soft-threshold parameter with high value (T=15 - T=19) will make the estimated image the highest PSNR.

For Speckle Noise, the Andrew's Sine norm soft-threshold parameter with high value (T=19) will make the estimated image the highest PSNR for low noise intensities and the Andrew's Sine norm soft-threshold parameter with low value (T=1) will make the estimated image the highest PSNR for high noise intensities, instead.

For Salt & Pepper Noise, the Andrew's Sine norm soft-threshold parameter with medium value (T=9) will make the estimated image the highest PSNR.

4.2 The comparative evaluation of simulation of a robust regularized SRR algorithm based on ML framework

In this section, the data processing simulations and their results are achieved by the SRR framework using the proposed Andrew's Sine norm estimation technique, which can be implemented by Eq. (9) and Eq. (10) respectively. To validate the achievement of the SRR algorithms using the proposed Andrew's Sine norm estimation technique, the estimated image from the SRR algorithm using the L1 norm estimation technique, which can be implemented by Eq. (4), and the estimated image of the SRR algorithm using the L1 norm estimation technique, which can be implemented by Eq. (6) are comparatively displayed for analyzing the performance.

This section presents the simulation results of the estimated images constituted by the SRR framework using the proposed Andrew's Sine norm estimation technique, the L1 norm estimation technique and the L2 norm estimation technique as shown in Figure 1 for Susie image and Figure 2 for Lena image, respectively. These simulation results consist of 5 noise models: Noiseless, Additive White Gaussian Noise (AWGN), Poisson Noise, Speckle Noise and Salt & Pepper Noise.

From the comparative simulation of the estimated Susie image as shown Figure 1, these comparatively simulated results are condensed as succeeding.

For Noiseless environment, the estimated images constituted by the SRR framework using the proposed Andrew's Sine norm estimation technique have the higher PSNR than the estimated images constituted by the SRR framework using the L1 norm estimation technique and the L2 norm estimation technique about 2.62dB and 0.58dB, respectively.

For AWGN environment, the estimated images constituted by the SRR framework using the proposed Andrew's Sine norm estimation technique have the higher PSNR than the estimated images constituted by the SRR framework using the L1 norm estimation technique and the L2 norm estimation technique about 1.90dB and 0.07dB, respectively.

For Poisson noise environment, the estimated images constituted by the SRR framework using the proposed Andrew's Sine norm estimation technique have the higher PSNR than the estimated images constituted by the SRR framework using the L1 norm estimation technique and the L2 norm estimation technique about 1.92dB and 0.07dB, respectively.

For Speckle noise environment, the estimated images constituted by the SRR framework using the proposed Andrew's Sine norm estimation technique have the higher PSNR than the estimated images constituted by the SRR framework using the L1 norm estimation technique and the L2 norm estimation technique about 1.27dB and 0.22dB, respectively.

For Salt & Pepper noise environment, the estimated images constituted by the SRR framework using the proposed Andrew's Sine norm estimation technique have the higher PSNR than the estimated images constituted by the SRR framework using the L1 norm estimation technique and the L2 norm estimation technique about 6.40dB and 4.43dB, respectively.

From the comparative simulation of the estimated Lena image as shown Figure 2, these comparatively simulated results are condensed as succeeding.

For Noiseless environment, the estimated images constituted by the SRR framework using the proposed Andrew's Sine norm estimation technique have the higher PSNR than the estimated images constituted by the SRR framework using the L1 norm estimation technique and the L2 norm estimation technique about 2.69dB and 0.70dB, respectively.

For AWGN environment, the estimated images constituted by the SRR framework using the proposed Andrew's Sine norm estimation technique have the higher PSNR than the estimated images constituted by the SRR framework using the L1 norm estimation technique and the L2 norm estimation technique about 1.57dB and 0.08dB, respectively.

For Poisson noise environment, the estimated images constituted by the SRR framework using the proposed Andrew's Sine norm estimation technique have the higher PSNR than the estimated images constituted by the SRR framework using the L1 norm estimation technique and the L2 norm estimation technique about 1.77dB and 0.01dB, respectively.

For Speckle noise environment, the estimated images constituted by the SRR framework using the proposed Andrew's Sine norm estimation technique have the higher PSNR than the estimated images constituted by the SRR

framework using the L1 norm estimation technique and the L2 norm estimation technique about 0.82dB and 0.32dB, respectively.

For Salt & Pepper noise environment, the estimated images constituted by the SRR framework using the proposed Andrew's Sine norm estimation technique have the higher PSNR than the estimated images constituted by the SRR framework using the L1 norm estimation technique and the L2 norm estimation technique about 4.77dB and 2.88dB, respectively.

For the performance analysis and conclusion, the proposed Andrew's Sine norm estimation gives the highest PSRN because this robust estimator is mathematically designed to be robust against noise and reject noise effectively. If the Andrew's Sine norm soft-threshold parameter is set to be low value (1-9) then the mathematical characteristic of the Andrew's Sine norm estimation is similar to L1 norm and, thus, this Andrew's Sine norm estimation can well suppress the impulse noise or high-power Gaussian noise (which has a long tail distribution). However, if the Andrew's Sine norm soft-threshold parameter is set to be high value (9-19) then the mathematical characteristic of the Andrew's Sine norm estimation is similar to L2 norm and, thus, this Andrew's Sine norm estimation can well suppress the low-power Gaussian noise (which has a quadratic distribution).

5. Conclusion

This paper presents the Andrew's Sine norm for a robust regularized SRR algorithm based on ML framework under various fraudulent blurred environments and aims to investigate the impact characteristic of this norm constant parameter on the novel SRR algorithm. A multitudinous experiments, which are applied on two standard images: Lena image and Susie image, are simulated to make the extensive results under five noise models: noise free, additive Gaussian noise, multiplicative Gaussian noise, Poisson noise and Impulsive noise with several noise powers for demonstrating the relationship between the SRR performance (in PSNR) and Andrew's Sine norm soft-threshold parameter under each noisy cases. Moreover, the comparative simulation of the estimated images constituted by the SRR framework using the proposed Andrew's Sine norm estimation technique, the L1 norm estimation technique and the L2 norm estimation technique are analyzed and discussed.

6. Notification

Portions of this research work were presented at the IEEE-NEWCAS-TAISA'08 Conference, 22-25 June 2008 as "Andrew's Sine Estimation for a Robust Iterative Multiframe Super-Resolution Reconstruction using Stochastic Regularization Technique" (Patanavijit, 2008).

7. Acknowledgement

The research project was funded by Assumption University.

8. References

Altunbasak, Y., Patti, A. J., & Mersereau, R. M. (2002). Super-resolution still and video reconstruction from MPEG-coded video. *IEEE Transactions on Circuits and Systems for Video Technology 12*(4), 217-226.

Black, M. J., Sapiro, G., Marimont, D., & Heeger, D. (1998). Robust anisotropic diffusion. *IEEE Transactions on Image Processing 7*(3), 421-432. DOI: 10.1109/83.661192

Elad, M., & Feuer, A. (1997). Restoration of a single superresolution image from several blurred, noisy, and undersampled measured images. *IEEE Transactions on Image Processing 6*(12), 1646-1658. DOI: 10.1109/83.650118

Elad, M., & Feuer, A. (1999a). Superresolution restoration of an image sequence: adaptive filtering approach. *IEEE Transactions on Image Processing 8*(3), 387-395. DOI: 10.1109/83.748893

Elad, M., & Feuer, A. (1999b). Super-resolution reconstruction of image sequences. *IEEE Transactions on Pattern Analysis and Machine Intelligence 21*(9), 817-834. DOI: 10.1109/34.790425

Elad, M., & Hel-Or, Y. (2001). A fast super-resolution reconstruction algorithm for pure translational motion and common space-invariant blur. *IEEE Transactions on Image Processing 10*(8), 1187-1193. DOI: 10.1109/83.935034

Farsiu, S., Robinson, M. D., Elad, M., & Milanfar, P. (2004a). Advances and challenges in super-resolution. *International Journal of Imaging Systems and Technology 14*(2), 47-57.

Farsiu, S., Robinson, M. D., Elad, M., & Milanfar, P. (2004b). Fast and robust multiframe

super resolution. *IEEE Transactions on Image Processing 13*(10), 1327-1344. DOI: 10.1109/TIP.2004.834669

Farsiu, S., Elad, M., & Milanfar, P. (2006). Multiframe demosaicing and super-resolution of color images. *IEEE Trans. on Image Processing 15*(1), 141-159. DOI: 10.1109/TIP.2005.860336

Kang, M. G., & Chaudhuri, S. (2003). Super-resolution image reconstruction. *IEEE Signal Processing Magazine 20*(3), 19-20.

Ng, M. K., & Bose, N. K. (2003). Mathematical analysis of super-resolution methodology. *IEEE Signal Processing Magazine 20*(3), 62-74. DOI: 10.1109/MSP.2003.1203210

Park, S. C., Park, M. K., & Kang, M. G. (2003). Super-resolution image reconstruction: a technical overview. *IEEE Signal Processing Magazine 20*(3), 21-36. DOI: 10.1109/MSP.2003.1203207

Patanavijit, V. (2008). Andrew's Sine estimation for a robust iterative multiframe super-resolution reconstruction using stochastic regularization technique. *Proceeding of IEEE Northeast Workshop on Circuits And Systems (IEEE-NEWCAS-TAISA'08)*, Montreal, Canada, June 2008.

Patanavijit, V. (2009a). Super-resolution reconstruction and its future research direction, *AU Journal of Technology (AU J.T.)*, Assumption University of Thailand, Bangkok, Thailand, Jan. 12(3), 149–163.

Patanavijit, V. (2009b). Mathematical analysis of stochastic regularization approach for super-resolution reconstruction, *AU Journal of Technology (AU J.T.)*, Assumption University of Thailand, Bangkok, Thailand, April. 12(4), 235–244.

Patanavijit, V. (2009c), A robust iterative multiframe SRR based on Andrew's Sine stochastice with Andrew's Sine-Tikhonov regularization, *Proceeding of IEEE International Symposium on Intelligent Signal Processing and Communication Systems (ISPACS 2008)*, Bangkok, Thailand, 8-11 Feb. 2009. Page(s): 1-4. DOI: 10.1109/ISPACS.2009.4806736

Patanavijit, V. (2009d), Video enhancement using a robust iterative SRR based on Andrew's Sine regularization technique, *Proceeding of IEEE International Symposium on Intelligent Signal Processing and Communication Systems (ISPACS 2009)*, Kanazawa, Japan, 7-9 Jan. 2009. Page(s): 115-118. DOI: 10.1109/ISPACS.2009.5383890

Patanavijit, V. (2011), A robust recursive SRR based on Andrew's Sine stochastic estimation with fast affine block-based registration for video enhancement, *Proceedings of The 34th Electrical Engineering Conference (EECON-34)*, Ambassador City Jomtien Hotel, Pataya, Chonburi, Thailand, Dec.

Patanavijit, V. (2013), Computational Tutorial of Steepest Descent Method and Its Implementation in Digital Image Processing, ECTI E-magazine, ECTI Association, Bangkok, Thailand, Vol. 7, No. 1, Jan. – Mar. (http://www.ecti-thailand.org/emagazine/) (ISSN: 2286-7074)

Patanavijit, V. (2015). Comparative experimental exploration of robust norm functions for iterative super resolution reconstructions under noise surrounding, *ECTI Transactions on EEC (Electrical Engineering/ Electronics and Communications)*, *13*(2), 83-91. ECTI Association, Thailand.

Patti, A. J., & Altunbasak, Y. (2001). Artifact reduction for set theoretic super resolution image reconstruction with edge constraints and higher-order interpolation. *IEEE Transactions on Image Processing 10*(1), 179-186.

Rajan, D., Chaudhuri, S., & Joshi, M. V. (2003). Multi-objective super resolution concepts and examples. *IEEE Signal Processing Magazine 20*(3), 49-61. DOI: 10.1109/MSP.2003.1203209

Rajan, D., & Chaudhuri, S. (2003). Simultaneous estimation of super-resolution scene and depth map from low resolution defocuses observations. *IEEE Transactions on Pattern Analysis and Machine Intelligence 25*(9), 1102-1117. DOI: 10.1109/TPAMI.2003.1227986

Schultz, R. R., & Stevenson, R. L. (1994). A Bayesian approach to image expansion for improved definition. *IEEE Transactions. on Image Processing 3*(3), 233-242. DOI: 10.1109/83.287017

Schultz, R. R., & Stevenson, R. L. (1996). Extraction of high-resolution frames from video sequences. *IEEE Transactions on Image Processing 5*(6), 996-1011. DOI: 10.1109/83.503915

Table 1 The result of simulation of Andrew's Sine norm soft-threshold parameter: Susie

Noise Case		**Reconstructed Frame in PSNR (dB)**					
	LR Frame	T=1	T=3	T=5	T=9	T=15	T=19
AWGN(dB)							
SNR=15	23.7086	27.6620	27.4148	27.1549	27.2353	27.6640	**27.7981**
SNR=17.5	25.7322	28.5888	28.5964	28.6473	28.9932	29.3362	**29.4251**
SNR=20	27.5316	29.3384	29.3978	29.7174	30.3485	30.6732	**30.7257**
SNR=22.5	29.0233	30.0635	30.2950	30.7352	31.3466	31.6561	**31.7038**
SNR=25	30.1214	30.6190	30.9682	31.5455	32.2125	32.3830	**32.3923**
Poisson	27.9071	29.5122	29.6164	29.8955	30.5684	30.8206	**30.8360**
S&P							
D=0.015	25.2760	29.8310	33.0566	34.1478	**34.4497**	34.3850	34.3199
D=0.010	26.4446	30.2021	33.3044	34.1644	**34.4742**	34.3911	34.3039
D=0.005	29.0649	30.6905	33.3987	34.1709	**34.4748**	34.4036	34.3313
Speckle:							
V:0.03	24.0403	**27.9403**	27.3321	26.6401	26.0474	26.6272	27.1227
V:0.02	25.3563	28.4431	27.9733	27.4849	27.3960	28.2785	**28.6021**
V:0.01	27.6166	29.3360	29.0953	28.9441	29.5950	30.2731	**30.4604**

Table 2 The result of simulation of Andrew's Sine norm soft-threshold parameter: Lena

Noise Case		**Reconstructed Frame in PSNR (dB)**					
	LR Frame	T=1	T=3	T=5	T=9	T=15	T=19
AWGN(dB)							
SNR=15	23.3549	25.8840	25.8361	25.8716	26.1665	26.5836	**26.7178**
SNR=17.5	24.9598	26.4827	26.5267	26.6818	27.2481	27.7853	**27.8765**
SNR=20	26.2188	27.0755	27.1926	27.5033	28.2051	28.5847	**28.6288**
SNR=22.5	27.2417	27.6598	27.8643	28.3188	28.9905	29.1901	**29.1980**
SNR=25	27.8884	28.0393	28.3576	28.9817	29.6253	**29.7392**	29.7237
Poisson	26.5116	27.6678	28.6500	28.6465	28.7297	**28.7317**	28.7311
S&P							
D=0.015	24.2190	26.9199	29.2651	30.7171	**30.9435**	30.8916	30.8395
D=0.010	25.2677	27.1170	29.4684	30.7406	**30.9482**	30.8964	30.8478
D=0.005	26.8577	27.5514	29.4768	30.7739	**30.9544**	30.8986	30.8519
Speckle:							
V:0.05	21.7994	**25.2729**	24.9494	24.4788	23.8764	23.9369	24.2293
V:0.04	22.6069	**25.5611**	25.2987	24.9174	24.5088	24.7634	25.1397
V:0.03	23.5294	25.8751	25.6623	25.3811	25.2204	25.7262	**26.1051**

RJAS Vol. 6 No. 1 Jan.-Jun. 2016, pp. 1-16
ISSN 2229-063X (Print)/ISSN 2392-554X (Online)

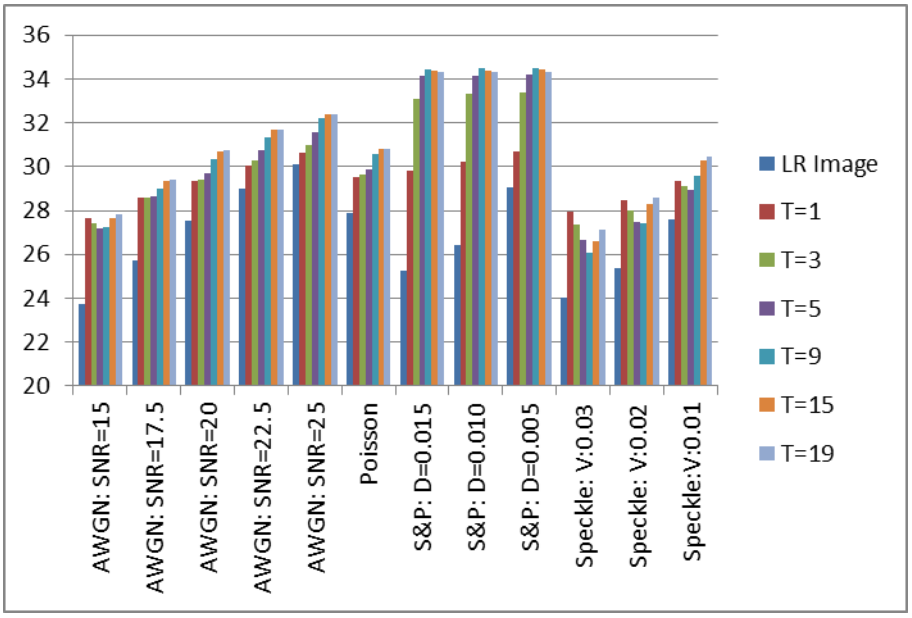

Figure 1 The result of simulation of Andrew's Sine norm soft-threshold parameter: SUSIE

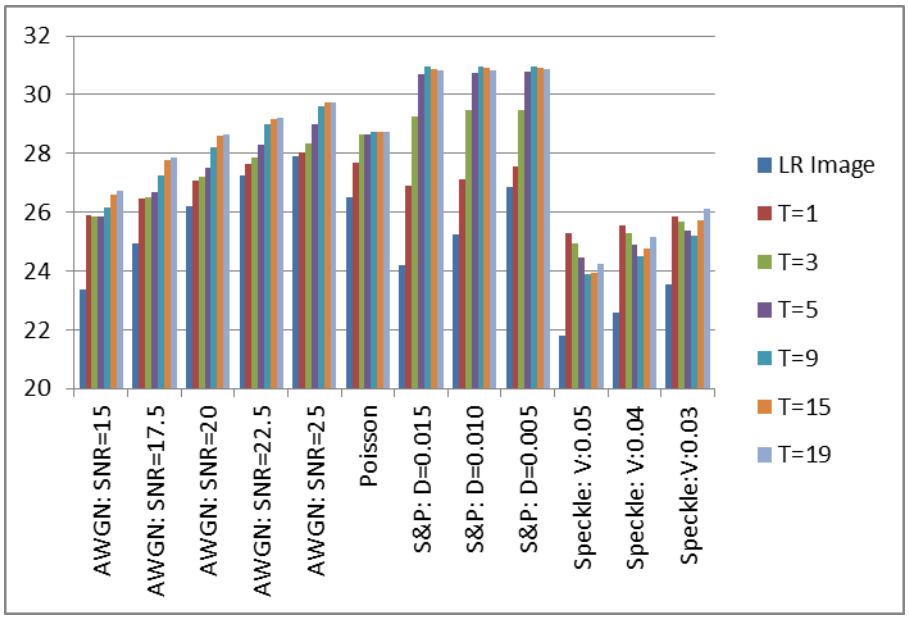

Figure 2 The result of simulation of Andrew's Sine norm soft-threshold parameter: LENA

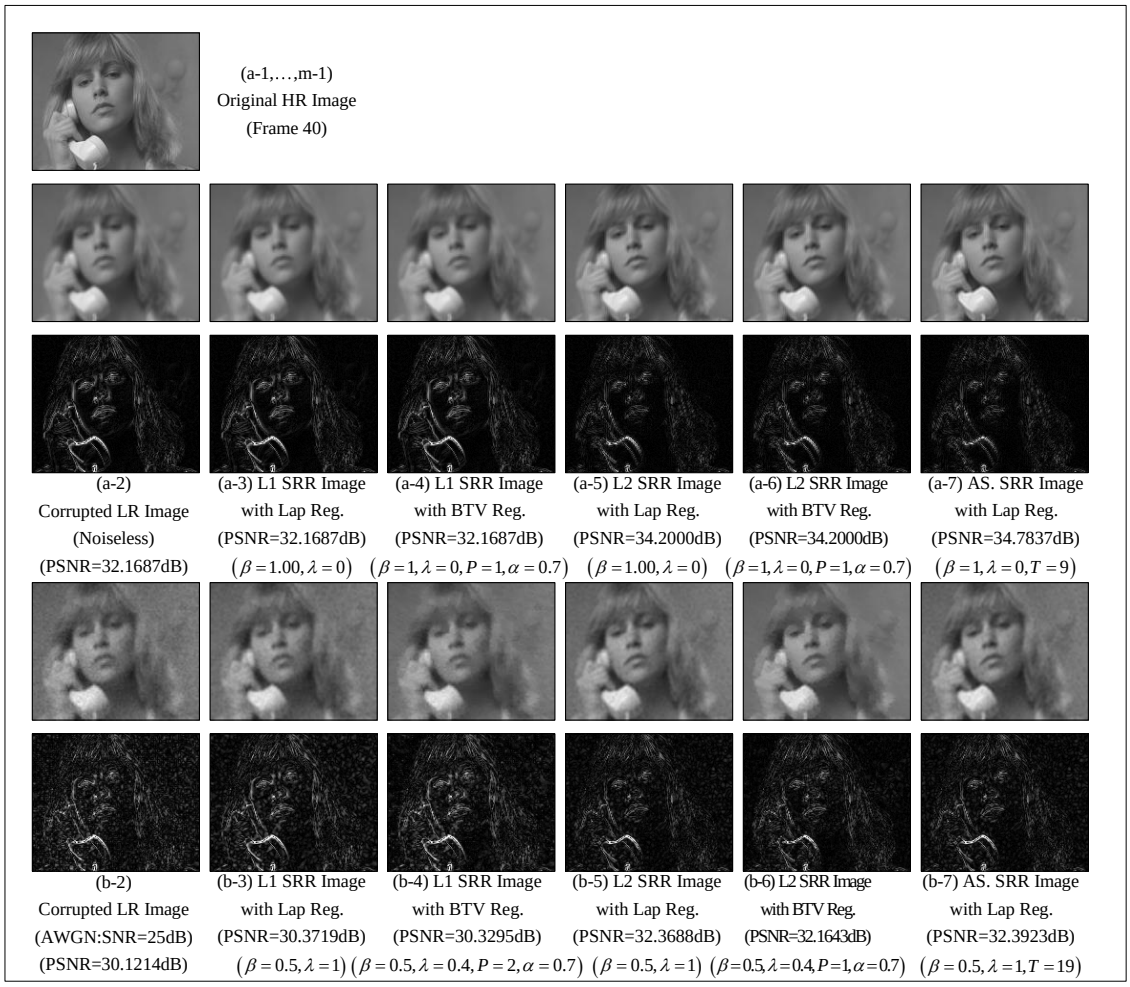

Figure 3 The estimated image from SRR simulation using proposed robust norm: Susie image (The beneath image on each estimated image of each subfigure is the absolute contrast, which is amplified by 5, between estimated image (at overhead) to the ground truth image) (BTV is the bilateral total variation regularization function [Farsiu, et al., 2004b])

Figure 3 The estimated image from SRR simulation using proposed robust norm: Susie image (The beneath image on each estimated image of each subfigure is the absolute contrast, which is amplified by 5, between estimated image (at overhead) to the ground truth image) (Cont.)

Figure 3 The estimated image from SRR simulation using proposed robust norm: Susie image (The beneath image on each estimated image of each subfigure is the absolute contrast, which is amplified by 5, between estimated image (at overhead) to the ground truth image) (Cont.)

Figure 3 The estimated image from SRR simulation using proposed robust norm: Susie image (The beneath image on each estimated image of each subfigure is the absolute contrast, which is amplified by 5, between estimated image (at overhead) to the ground truth image) (Cont.)

Figure 4 The estimated image from SRR simulation using proposed robust norm: Lena image (The beneath image on each estimated image of each subfigure is the absolute contrast, which is amplified by 5, between estimated image (at overhead) to the ground truth image)

Figure 4 The estimated image from SRR simulation using proposed robust norm: Lena image (The beneath image on each estimated image of each subfigure is the absolute contrast, which is amplified by 5, between estimated image (at overhead) to the ground truth image) (Cont.)

Figure 4 The estimated image from SRR simulation using proposed robust norm: Lena image (The beneath image on each estimated image of each subfigure is the absolute contrast, which is amplified by 5, between estimated image (at overhead) to the ground truth image) (Cont.)